

## On the Mechanism of Homogeneous Decomposition of the Chlorinated Silanes. Chain Reactions Propagated by Divalent Silicon Species

Mark T. Swihart\* and Robert W. Carr

Department of Chemical Engineering and Materials Science, University of Minnesota,  
Minneapolis, Minnesota 55455

Received: September 30, 1997; In Final Form: January 6, 1998

A mechanism for the homogeneous gas-phase decomposition of  $\text{SiHCl}_3$ ,  $\text{SiH}_2\text{Cl}_2$ , and  $\text{SiH}_3\text{Cl}$  in hydrogen is derived from the results of ab initio molecular-orbital studies. It consists of 39 reversible elementary reactions among 25 species, including pressure-dependent unimolecular decomposition of the chlorinated silanes and secondary chemistry due to reactions of  $\text{SiH}_2$ ,  $\text{SiHCl}$ , and  $\text{SiCl}_2$  with one another and with the chlorinated silanes. Rate parameters in the mechanism have been calculated based on results of ab initio studies using transition-state theory and unimolecular rate theories. This allows us to construct a reasonably complete mechanism that provides qualitative explanations for several features of dichlorosilane decomposition that have been presented in the literature, including observations on the presence and concentrations of  $\text{SiCl}_2$ ,  $\text{SiHCl}$ , and Si atoms. Several chain reactions in which the chain carriers are divalent silicon species have been identified.

### Introduction

The chlorinated silanes, particularly dichlorosilane and trichlorosilane, are used as precursors for the chemical vapor deposition (CVD) of epitaxial silicon. At the high temperatures where this process is carried out, homogeneous decomposition of the parent molecules may play an important role by generating reactive species that lead to film growth. Secondary reactions can both accelerate the decomposition of the precursor and consume reactive intermediates that could otherwise lead to film growth. To understand the mechanisms of film growth and develop detailed, physically based models of silicon epitaxy from the chlorinated silanes, we must be able to assess which, if any, homogeneous reactions are likely to be important at the reactor conditions and what the rates of these reactions are. This has not, so far, been possible for silicon epitaxy from dichlorosilane or trichlorosilane. Here, we present a reaction mechanism and rate parameters for the homogeneous thermal decomposition of the chlorinated silanes. The mechanism is applicable to homogeneous decomposition of  $\text{SiH}_3\text{Cl}$ ,  $\text{SiH}_2\text{Cl}_2$ , and  $\text{SiHCl}_3$  in  $\text{H}_2$ . Silane decomposition mechanisms are understood in more detail and have been presented and discussed elsewhere.<sup>1–3</sup> Additional chemical species and reactions would be required to describe  $\text{SiCl}_4$  decomposition.

A number of observations on thermal decomposition of the chlorosilanes have been published, but rate parameters and decomposition mechanisms have not been experimentally established. Laser pyrolysis of trichlorosilane<sup>4</sup> was observed to give HCl and a white powder that was assumed to result from  $\text{SiCl}_2$  polymerization. Rate parameters were obtained and were presumed to correspond to the elementary reaction  $\text{SiHCl}_3 \rightarrow \text{SiCl}_2 + \text{HCl}$ . There are several observations of dichlorosilane decomposition in the literature, but both the rate parameters and the primary reaction products still remain somewhat unclear. In IR multiphoton dissociation experiments, Sausa and Ronn<sup>5</sup> detected electronically excited  $\text{SiCl}_2$ . Walker et al.<sup>6</sup> decomposed monochlorosilane and trichlorosilane in static bulb experiments, and dichlorosilane both in static pyrolysis experiments and using

a single-pulse shock tube. They concluded that the initial dichlorosilane decomposition products were  $\text{SiCl}_2$  and  $\text{H}_2$ , based partially on the fact that very little HCl was observed as a product in their shock-tube experiments. They interpreted their experimental results in terms of a reaction mechanism that differs in some respects from the one presented here. On the basis of that mechanism, they obtain rate parameters for the three decompositions. Kruppa, Shin, and Beauchamp<sup>7</sup> found that  $\text{SiCl}_2$  and HCl were the primary products of vacuum flash pyrolysis of  $\text{SiH}_2\text{Cl}_2$ . Ban and Gilbert<sup>8</sup> observed  $\text{SiCl}_2$  by mass spectrometry under silicon CVD conditions, and Ho and Breiland<sup>9</sup> observed  $\text{SiHCl}$  by laser-induced fluorescence in a silicon CVD reactor. Ho, Breiland, and Carr<sup>10</sup> observed that 193-nm photolysis of  $\text{SiH}_2\text{Cl}_2$  produced  $\text{SiHCl}$ . In pulsed laser-powered homogeneous pyrolysis experiments,<sup>11</sup> we measured reaction rates consistent with an activation energy for unimolecular decomposition near 75 kcal/mol but were unable to identify the primary reaction products.

Ab initio calculations<sup>12,13</sup> predict that the dominant unimolecular decomposition path for dichlorosilane is  $\text{SiH}_2\text{Cl}_2 \rightarrow \text{SiHCl} + \text{HCl}$ , with an activation energy near 75 kcal/mol. CVD reactor models that included reactions in the gas phase<sup>14,15</sup> have assumed that the reaction was  $\text{SiH}_2\text{Cl}_2 \rightarrow \text{SiCl}_2 + \text{H}_2$ . These models also used rate parameters that gave reaction rates that were orders of magnitude larger than the rates of the unimolecular decomposition reactions predicted from the ab initio calculations. This apparent discrepancy could be partially resolved if there are secondary reactions in the gas phase that accelerate the overall decomposition and convert  $\text{SiHCl}$  to  $\text{SiCl}_2$ . Consideration of such mechanisms can also shed light on the varied experimental observations of dichlorosilane decomposition and on related processes in the decomposition of monochlorosilane and trichlorosilane.

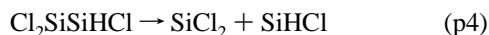
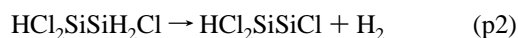
In this work, we present a mechanism and rate parameters based on ab initio calculations for the unimolecular decomposition reactions of the chlorinated silanes and subsequent second-

TABLE 1: Reaction Mechanism and Rate Parameters<sup>a</sup>

	reaction	log $A_\infty$	$E_\infty$	log $A_0$	$E_0$	$T^{***}$	$T^{**}$	$\Delta S_{1000}^0$	$\Delta H_{1000}^0$
(1)	$\text{SiH}_4 \leftrightarrow \text{SiH}_2 + \text{H}_2$	14.7	60.5	-7.1	51.5	1090	7210	34.3	58.0
(2)	$\text{SiH}_3\text{Cl} \leftrightarrow \text{SiHCl} + \text{H}_2$	15.0	68.9	-6.6	57.6	710	3150	33.3	47.9
(3)	$\text{SiH}_2\text{Cl}_2 \leftrightarrow \text{SiHCl} + \text{HCl}$	14.9	75.0	-6.3	62.0	540	3040	35.6	66.7
(4)	$\text{SiH}_2\text{Cl}_2 \leftrightarrow \text{SiCl}_2 + \text{H}_2$	13.9	76.6	-9.6	64.2	<i>b</i>	<i>b</i>	31.6	36.4
(5)	$\text{SiHCl}_3 \leftrightarrow \text{SiCl}_2 + \text{HCl}$	14.7	71.7	-6.4	56.7	430	3051	35.8	55.4
(6)	$\text{H}_3\text{SiSiH}_3 \leftrightarrow \text{SiH}_4 + \text{SiH}_2$	14.5	45.6					30.5	52.4
(7)	$\text{H}_3\text{SiSiH}_3 \leftrightarrow \text{Si}_2\text{H}_4 + \text{H}_2$	14.7	55.0					32.2	49.8
(8)	$\text{H}_2\text{ClSiSiH}_3 \leftrightarrow \text{SiH}_3\text{Cl} + \text{SiH}_2$	14.2	47.3					29.8	52.3
(9)	$\text{H}_2\text{ClSiSiH}_3 \leftrightarrow \text{SiH}_4 + \text{SiHCl}$	13.4	48.8					28.8	42.2
(10)	$\text{H}_2\text{ClSiSiH}_3 \leftrightarrow \text{Si}_2\text{H}_3\text{Cl} + \text{H}_2$	14.4	53.9					32.4	48.4
(11)	$\text{H}_2\text{ClSiSiH}_2\text{Cl} \leftrightarrow \text{SiH}_2\text{Cl}_2 + \text{SiH}_2$	13.1	47.6					31.8	50.3
(12)	$\text{H}_2\text{ClSiSiH}_2\text{Cl} \leftrightarrow \text{SiH}_3\text{Cl} + \text{SiHCl}$	13.8	45.3					32.9	42.2
(13)	$\text{H}_2\text{ClSiSiH}_2\text{Cl} \leftrightarrow \text{Si}_2\text{H}_2\text{Cl}_2 + \text{H}_2$	14.5	54.2					33.1	47.2
(14)	$\text{HCl}_2\text{SiSiH}_3 \leftrightarrow \text{SiH}_2\text{Cl}_2 + \text{SiH}_2$	14.1	49.8					30.7	52.7
(15)	$\text{HCl}_2\text{SiSiH}_3 \leftrightarrow \text{SiH}_3\text{Cl} + \text{SiHCl}$	13.8	52.1					31.8	44.6
(16)	$\text{HCl}_2\text{SiSiH}_3 \leftrightarrow \text{SiH}_4 + \text{SiCl}_2$	13.3	53.8					28.1	31.1
(17)	$\text{HCl}_2\text{SiSiH}_3 \leftrightarrow \text{Si}_2\text{H}_2\text{Cl}_2 + \text{H}_2$	14.4	53.5					32.0	49.6
(18)	$\text{HCl}_2\text{SiSiH}_2\text{Cl} \leftrightarrow \text{SiHCl}_3 + \text{SiH}_2$	13.1	50.9					29.6	50.6
(19)	$\text{HCl}_2\text{SiSiH}_2\text{Cl} \leftrightarrow \text{SiH}_2\text{Cl}_2 + \text{SiHCl}$	13.6	46.9					32.5	42.7
(20)	$\text{HCl}_2\text{SiSiH}_2\text{Cl} \leftrightarrow \text{SiH}_3\text{Cl} + \text{SiCl}_2$	13.1	49.3					30.8	31.1
(21)	$\text{HCl}_2\text{SiSiH}_2\text{Cl} \leftrightarrow \text{Si}_2\text{HCl}_3 + \text{H}_2$	13.9	54.9					32.9	46.0
(22)	$\text{Cl}_3\text{SiSiH}_3 \leftrightarrow \text{SiHCl}_3 + \text{SiH}_2$	14.1	51.3					32.3	54.1
(23)	$\text{Cl}_3\text{SiSiH}_3 \leftrightarrow \text{SiH}_3\text{Cl} + \text{SiCl}_2$	14.1	49.6					33.5	34.7
(24)	$\text{Cl}_3\text{SiSiH}_3 \leftrightarrow \text{Si}_2\text{HCl}_3 + \text{H}_2$	14.3	53.5					35.6	49.5
(25)	$\text{HCl}_2\text{SiSiHCl}_2 \leftrightarrow \text{SiHCl}_3 + \text{SiHCl}$	13.7	47.7					32.8	42.8
(26)	$\text{HCl}_2\text{SiSiHCl}_2 \leftrightarrow \text{SiH}_2\text{Cl}_2 + \text{SiCl}_2$	13.3	51.7					33.0	31.5
(27)	$\text{Cl}_3\text{SiSiH}_2\text{Cl} \leftrightarrow \text{SiCl}_4 + \text{SiH}_2$	13.2	55.5					22.0	51.6
(28)	$\text{Cl}_3\text{SiSiH}_2\text{Cl} \leftrightarrow \text{SiHCl}_3 + \text{SiHCl}$	13.5	49.8					32.1	43.7
(29)	$\text{Cl}_3\text{SiSiH}_2\text{Cl} \leftrightarrow \text{SiH}_2\text{Cl}_2 + \text{SiCl}_2$	13.8	44.3					32.3	32.4
(30)	$\text{Cl}_3\text{SiSiH}_2\text{Cl} \leftrightarrow \text{Si}_2\text{Cl}_4 + \text{H}_2$	14.4	55.0					34.3	45.4
(31)	$\text{Cl}_3\text{SiSiHCl}_2 \leftrightarrow \text{SiCl}_4 + \text{SiHCl}$	13.7	52.3					24.4	43.6
(32)	$\text{Cl}_3\text{SiSiHCl}_2 \leftrightarrow \text{SiHCl}_3 + \text{SiCl}_2$	13.9	45.9					31.8	32.4
(33)	$\text{Cl}_3\text{SiSiCl}_3 \leftrightarrow \text{SiCl}_4 + \text{SiCl}_2$	14.2	48.8					28.1	33.2
(34)	$\text{Si}_2\text{H}_4 \leftrightarrow 2\text{SiH}_2$	15.0	60.6					32.6	60.6
(35)	$\text{Si}_2\text{H}_3\text{Cl} \leftrightarrow \text{SiH}_2 + \text{SiHCl}$	15.0	51.9					30.7	51.9
(36)	$\text{Si}_2\text{H}_2\text{Cl}_2 \leftrightarrow \text{SiH}_2 + \text{SiCl}_2$	15.0	39.5					30.4	39.5
(37)	$\text{Si}_2\text{H}_2\text{Cl}_2 \leftrightarrow 2\text{SiHCl}$	15.0	42.9					33.1	42.9
(38)	$\text{Si}_2\text{HCl}_3 \leftrightarrow \text{SiHCl} + \text{SiCl}_2$	15.0	33.1					31.3	33.1
(39)	$\text{Si}_2\text{Cl}_4 \leftrightarrow 2\text{SiCl}_2$	15.0	23.4					29.7	23.4

<sup>a</sup>  $A_\infty$  in  $\text{s}^{-1}$ ,  $E_\infty$ ,  $E_0$ , and  $\Delta H$  in kcal/mol.  $A_0$  in  $\text{cm}^3/(\text{molecule s})$ .  $T^{***}$  and  $T^{**}$  in K.  $\Delta S$  in cal/(mol K). Rate parameters have been calculated or estimated as described in the text.  $\Delta H$  and  $\Delta S$  are the enthalpy and entropy changes on reaction at 1000 K and 1 atm, calculated as described in the text. <sup>b</sup> This channel for dichlorosilane decomposition cannot be parametrized by the standard Troe fit. Its falloff behavior is strongly influenced by the dominant channel eq 3 such that this channel would require a broadening factor  $F > 1$  over a large range of pressures.

ary chemistry involving the chlorinated silylenes, silylsilylenes, disilenes, and disilanes. Several chain mechanisms with divalent silicon species as the chain carriers can be identified within the overall mechanism. An example of a chain mechanism for dichlorosilane decomposition is



An alternative mechanism would replace steps p2–p4 with



which lead to the same overall reaction. Clearly, we could write many similar reactions and cycles involving the other chlorinated silanes and their decomposition products, and the number of

variations and combinations would become quite large. The importance of different reaction paths will depend on such things as the branching ratios for the decompositions of the chlorinated disilanes (i.e., eq p2 vs eq p5 vs the reverse of eq p1) and rates of insertion of the chlorinated silylenes into the parent chlorinated silanes. The goals of this work are to develop a reaction mechanism that includes chain mechanisms such as those presented above and to examine the implications of this mechanism for chlorinated silane decomposition under various conditions of relevance to epitaxial growth of silicon. We show that this mechanism provides an explanation for some experimental observations of  $\text{SiCl}_2$ ,  $\text{SiHCl}$ , and  $\text{Si}$  atoms in dichlorosilane decomposition and silicon epitaxy from dichlorosilane.

## Mechanism

The reaction mechanism considered in this work is presented in Table 1. The choice of reactions to be included or excluded and the means of calculating rate parameters are presented and discussed in this section. The mechanism consists of 39 reversible reactions among 25 distinct species. The species considered are  $\text{H}_2$ ,  $\text{HCl}$ , the silylenes ( $\text{SiH}_2$ ,  $\text{SiHCl}$ ,  $\text{SiCl}_2$ ), the silanes ( $\text{SiH}_n\text{Cl}_{4-n}$ ), the disilanes ( $\text{Si}_2\text{H}_n\text{Cl}_{6-n}$ ), and six compounds with stoichiometry  $\text{Si}_2\text{H}_n\text{Cl}_{4-n}$  (silylsilylenes or disilenes). Reactions 1–5 are the unimolecular decompositions

of the monosilanes ( $\text{SiH}_n\text{Cl}_{4-n}$ ) and their reverse reactions, insertion of  $\text{SiH}_2$ ,  $\text{SiHCl}$ , and  $\text{SiCl}_2$  into  $\text{H}_2$  and  $\text{HCl}$ . Reactions 6–33 are the unimolecular elimination of  $\text{SiH}_2$ ,  $\text{SiHCl}$ ,  $\text{SiCl}_2$ , and  $\text{H}_2$  from the chlorinated disilanes. The chlorinated disilanes are formed by the reverse of these reactions. Reactions 34–39 are the unimolecular decompositions of chlorinated silylsilylenes or disilenes (see below) to give two chlorinated silylenes.

Simple bond-breaking reactions are not important for any of the silanes or disilanes in the mechanism. The Si–H bond strength is about 93 kcal/mol, the Si–Cl bond strength is about 110 kcal/mol, and the Si–Si bond strength in the disilanes is about 77 kcal/mol. Thus, these reactions cannot compete with the alternative hydrogen and  $\text{HCl}$  eliminations from the chlorinated silanes or the silylene and hydrogen eliminations from the chlorinated disilanes and are not included. Likewise, we do not consider  $\text{HCl}$  or  $\text{Cl}_2$  elimination from the chlorinated disilanes because these reactions are roughly 75 and 135 kcal/mol endothermic, respectively, and cannot compete with the silylene- and hydrogen-elimination reactions. We have not included any reactions leading to higher chlorinated silanes (species with three or more silicon atoms), such as dimerization of the  $\text{Si}_2\text{H}_n\text{Cl}_{4-n}$  species, insertion of silylsilylenes into silanes, or insertion of silylenes into disilanes. Formation of polychlorosilanes by one or more of these mechanisms could be the first step toward formation of particles by a polymerization process. However, at temperatures high enough for significant decomposition of the chlorinated silanes to occur, the two-silicon-containing molecules involved in these reactions are present at much lower concentrations than the molecules with one silicon atom. This reflects the fact that the two-silicon-containing molecules have fast unimolecular decomposition paths available to them so that bimolecular reactions leading to higher polychlorosilanes are not important in determining their rates of consumption.

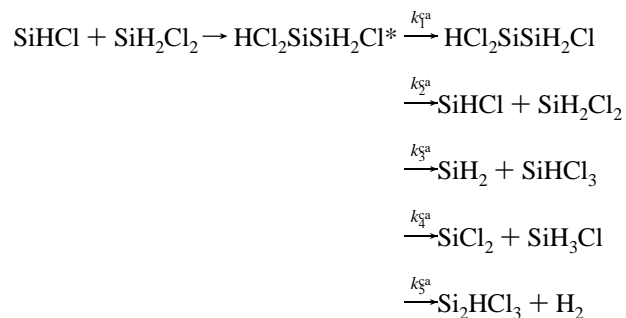
Forward rate parameters for each reaction are presented. Reverse rate parameters were calculated from the equilibrium constant obtained from the  $\Delta H^\circ$  and  $\Delta S^\circ$  of reaction. The enthalpy and entropy changes were treated as constant at the values at 1000 K presented in Table 1. Heats of formation of reactants and products at 298 K were taken from ab initio calculations<sup>14,15</sup> that agreed well with experimental values where comparison was possible. Entropies and enthalpies at 1000 K were obtained using the vibrational frequencies and moments of inertia from the ab initio calculations at the MP2/6-31G-(d,p) level.<sup>14,15</sup> Standard statistical mechanical formulas<sup>16</sup> were used. For the few reactions for which heats of formation of reactants and products are available from other sources, the resulting  $\Delta H^\circ$  and  $\Delta S^\circ$  of reaction calculated here agree well. For example, the values from the JANAF tables<sup>17</sup> would give  $\Delta H^\circ = 36.7$  kcal/mol and  $\Delta S^\circ = 31.3$  cal/(mol K) for reaction 5, compared with our values of  $\Delta H^\circ = 36.4$  kcal/mol and  $\Delta S^\circ = 31.6$  cal/(mol K).

**Pressure-Dependent Unimolecular Decomposition of the Chlorinated Silanes.** Rate parameters for reactions 1–5 were based on the ab initio structures, energetics, and vibrational frequencies for reactants, products, and transition states presented by Schlegel et al.<sup>12,14</sup> They have presented higher-level calculations<sup>13</sup> for dichlorosilane decomposition (reactions 4 and 5), but the changes from the previous study were small. The results from the earlier publication were used for the sake of consistency of treatment with other reactions considered here. Higher-energy decomposition paths, such as  $\text{SiH}_3\text{Cl} \rightarrow \text{SiH}_2 + \text{HCl}$ , were not included. Reactions 1–5 are in the pressure-dependent unimolecular falloff regime under conditions of

interest. Master-equation calculations were performed to obtain the pressure-dependent rate parameters for these reactions in hydrogen carrier gas. The UNIMOL suite of programs by Gilbert et al.<sup>18</sup> was used for these calculations. There is no experimental information on energy transfer in this system, so an estimate was made by comparison with similar systems at high temperature.<sup>19,20</sup> An exponential model for the energy-transfer probability function was used<sup>21,22</sup> with  $\langle \Delta E \rangle_d = 0.55$  kcal/mol ( $192 \text{ cm}^{-1}$ ). The results are presented in Table 1 as simplified Troe parametrizations.<sup>23</sup> The parameters presented in Table 1 were obtained by fitting these expressions to the master-equation calculations over the temperature range 800–1300 K. Reaction 4, the minor decomposition channel for dichlorosilane, cannot readily be fit to the Troe form. Its falloff behavior is strongly influenced by the major channel (reaction 3) such that it would require  $F > 1$  and with a different functional form. Reaction 1, silane decomposition, has been studied experimentally, but there is not universal agreement on the rate parameters.<sup>24</sup> Our calculated rate parameters are comparable to those from an analysis of several of the experimental results by Moffat et al.<sup>25</sup> In the high-pressure limit at 1100 K, our ab initio based calculations give an activation energy that is 0.5 kcal/mol higher and a preexponential factor that is an order of magnitude lower than that given by Moffat. There are substantial uncertainties in both estimates. There are no published experimental results with which to compare the rate parameters for the other reactions.

**Reactions Involving the Chlorinated Disilanes and Treatment of Chemically Activated Reactions.** Rate parameters for reactions 6–33 are based on the structures, energetics, and vibrational frequencies from ab initio molecular-orbital calculations.<sup>15</sup> These ab initio calculations used the same methodology as those upon which reactions 1–5 are based. For reactions 6–33, only high-pressure-limiting rate parameters are given. These were obtained using conventional transition-state theory.<sup>26</sup> At the relatively high temperatures considered here, this tight transition-state treatment works reasonably well even for the reactions where the insertion has a negative activation energy. However, at lower temperatures a variational treatment with a loose transition state would be required. A discussion of these reactions and comparison of the rate parameters with the scant experimental information that is available are given in our previous work.<sup>15</sup>

We have not treated the pressure dependence of these reactions. Doing so would not only require multichannel RRKM or master-equation falloff calculations for the decomposition reactions but would also require explicit treatment of the recombination reactions as multichannel chemically activated processes. Analysis of the  $\text{SiHCl} + \text{SiH}_2\text{Cl}_2$  reaction, presented in detail below, shows that this is not necessary under conditions of interest here. This chemically activated reaction may be written as



where  $\text{HCl}_2\text{SiSiH}_2\text{Cl}^*$  indicates chemically activated 1,1,2-

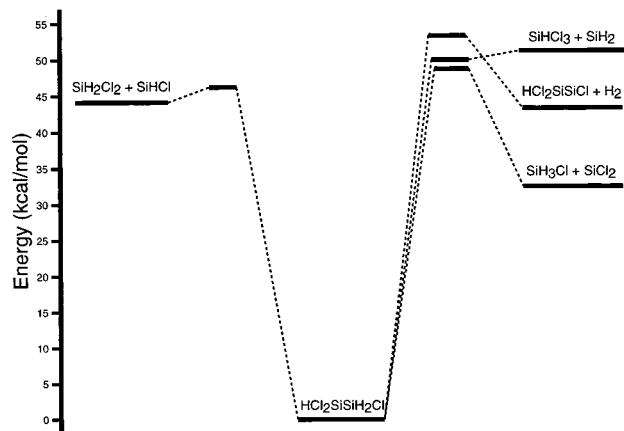


**Figure 1.** Energetics of the chemically activated system described in the text. Energies of reactants, products, and transition states are electronic plus zero-point energies from ab initio calculations<sup>16</sup> relative to  $\text{HCl}_2\text{SiSiH}_2\text{Cl}$ .

trichlorodisilane that can either be collisionally stabilized or decompose by the four other channels shown. The rate coefficients  $k_1^{\text{ca}}-k_5^{\text{ca}}$  are composite second-order rate coefficients for the overall reaction and are composed of rate coefficients for the elementary bimolecular and unimolecular steps in the mechanism. The composite second-order rate coefficients are pressure-dependent. At high pressures, collisional stabilization (channel 1) dominates. As the pressure falls, collisional stabilization becomes slower and the other channels become important. The total rate, given by the sum of all five channels, including dissociation back to the reactants (channel 2), is independent of pressure. Figure 1 shows schematically the energetics of this system.

Master-equation calculations for this multichannel chemically activated system have been carried out, and we present and discuss them here both as an example of how a thorough and rigorous treatment of this system might be approached and to explore the approximations we are making by using only the high-pressure recombination and dissociation reactions for steps 6–33 in the mechanism presented here. This particular reaction is taken to be representative of the many similar chemically activated reactions that could be formally treated as such in this mechanism. Figure 2 shows calculated rate constants versus pressure for the five channels at 1100 K. Again, the bath gas is hydrogen and  $\langle\Delta E\rangle_d$  in the exponential model for the energy-transfer probability function was taken to be 0.55 kcal/mol (192  $\text{cm}^{-1}$ ). The methodology used for these calculations is described by Venkatesh et al.<sup>27,28</sup> We see that at this temperature with the energy-transfer and rate parameters used here, channel 2 (decomposition back to the reactants) dominates below about 100 Torr and channel 1 (recombination) dominates above this pressure. This transition moves to higher pressures with increasing temperature and to lower pressures with decreasing temperature. The pressure dependence of channels 2–5 is seen to be essentially the same. This is an important result because it means that the branching ratios between these four channels will not change much with pressure. This is discussed further below.

At temperatures and pressures considered in this work, the 1,1,2-trichlorodisilane produced by channel 1 (recombination) decomposes very rapidly compared to the overall time scale of reaction. In dichlorosilane-decomposition simulations, concentrations of the chlorinated disilanes are consistently 4–5 orders of magnitude smaller than the initial dichlorosilane concentrations. Thus, the 1,1,2-trichlorodisilane serves only as a channel

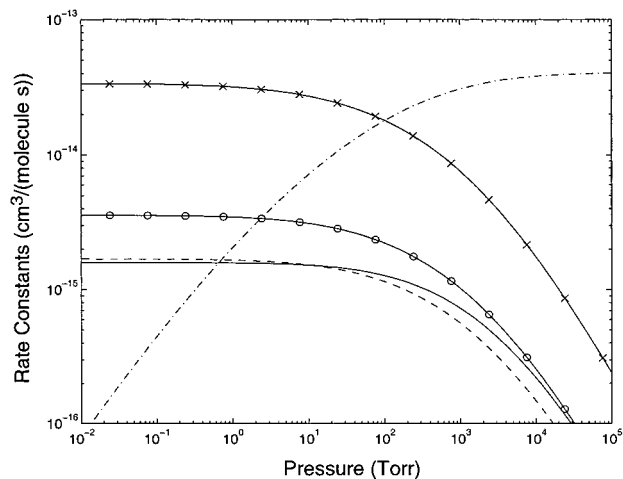


**Figure 2.** Second-order rate constants from master-equation calculations for the chemically activated system described in the text. The dash-dot line is  $k_1^{\text{ca}}$ , the  $\times$ 's are  $k_2^{\text{ca}}$ , the dashed line is  $k_3^{\text{ca}}$ , the  $\circ$ 's are  $k_4^{\text{ca}}$ , and the solid line is  $k_5^{\text{ca}}$ .

for conversion between  $\text{SiH}_2\text{Cl}_2 + \text{SiHCl}$  and the other possible sets of 1,1,2-trichlorodisilane decomposition products. In the high-pressure limit, this occurs entirely by bimolecular recombination (the reverse of reaction 19) followed by unimolecular decomposition (reactions 18–21). In the low-pressure limit, it occurs entirely by channels 2–5 of the chemically activated reaction system described above. At intermediate pressures, both processes occur. At high pressure, effective branching ratios for production of the four sets of bimolecular products (including the reactants) from reaction of  $\text{SiH}_2\text{Cl}_2 + \text{SiHCl}$  are simply the ratios of their decomposition rate constants. If 1,1,2-trichlorodisilane decomposes rapidly so that its concentration is always small, then it can be shown that the effective rate constant for production of a set of bimolecular products from  $\text{SiHCl} + \text{SiH}_2\text{Cl}_2$  is the recombination rate constant multiplied by the fraction of unimolecular decomposition that goes to that set of products. For example, the effective bimolecular rate constant at high pressure with rapid decomposition of  $\text{HCl}_2\text{-SiSiH}_2\text{Cl}$  for the overall reaction  $\text{SiH}_2\text{Cl}_2 + \text{SiHCl} \rightarrow \text{SiH}_3\text{Cl} + \text{SiCl}_2$  is given by

$$k_{\text{eff}} = k_{-19} \left( \frac{k_{20}}{k_{18} + k_{19} + k_{20} + k_{21}} \right)$$

where the numbers on the rate constants refer to reaction numbers in Table 1 and  $k_{-19}$  indicates the reverse of reaction 19. This expression can be obtained by applying a pseudo-steady-state approximation to the concentration of  $\text{HCl}_2\text{-SiSiH}_2\text{-Cl}$ . The rate constants in this expression are the high-pressure-limiting rate constants, and this behavior is what is given by the mechanism in Table 1 where high-pressure rate constants for recombination and decomposition are used, while chemically activated reactions are left out. The effective branching ratio for production of  $\text{SiH}_3\text{Cl} + \text{SiCl}_2$  from  $\text{SiH}_2\text{Cl}_2 + \text{SiHCl}$ , defined as the rate of production of  $\text{SiH}_3\text{Cl} + \text{SiCl}_2$  divided by the total rate of reaction of  $\text{SiH}_2\text{Cl}_2 + \text{SiHCl}$ , is then given by the expression inside the brackets. In the high-pressure limit with rapid decomposition of  $\text{HCl}_2\text{-SiSiH}_2\text{Cl}$ , then, the effective branching ratios for the four sets of products (including dissociation back to reactants) are

$$\begin{aligned}
 B_{2,\infty} &= \frac{\text{rate of production of SiH}_2\text{Cl}_2 + \text{SiHCl}}{\text{total rate of SiH}_2\text{Cl}_2 + \text{SiHCl reaction}} \\
 &= \frac{k_{19}}{k_{18} + k_{19} + k_{20} + k_{21}} \\
 B_{3,\infty} &= \frac{\text{rate of production of SiHCl}_3 + \text{SiH}_2}{\text{total rate of SiH}_2\text{Cl}_2 + \text{SiHCl reaction}} \\
 &= \frac{k_{18}}{k_{18} + k_{19} + k_{20} + k_{21}} \\
 B_{4,\infty} &= \frac{\text{rate of production of SiH}_3\text{Cl} + \text{SiCl}_2}{\text{total rate of SiH}_2\text{Cl}_2 + \text{SiHCl reaction}} \\
 &= \frac{k_{20}}{k_{18} + k_{19} + k_{20} + k_{21}} \\
 B_{5,\infty} &= \frac{\text{rate of production of Si}_2\text{HCl}_3 + \text{H}_2}{\text{total rate of SiH}_2\text{Cl}_2 + \text{SiHCl reaction}} \\
 &= \frac{k_{21}}{k_{18} + k_{19} + k_{20} + k_{21}}
 \end{aligned}$$

The numbering of the branching ratios is chosen to correspond to the numbering of the channels of the chemically activated reactions.  $B_{2,\infty}$  is the fraction of reacting  $\text{SiH}_2\text{Cl}_2 + \text{SiHCl}$  that dissociates back to the reactants,  $B_{3,\infty}$  is the fraction that dissociates to  $\text{SiHCl}_3 + \text{SiH}_2$ , etc. These are the effective branching ratios in the high-pressure limit under conditions where the 1,1,2-trichlorodisilane decomposes rapidly compared with the rate of change of species concentrations in the system.

At low pressures the dominant reactions are channels 2–5 of the chemically activated system presented above. We may similarly define branching ratios for the amount of reaction occurring by these channels as

$$B_i = \frac{k_i^{\text{ca}}}{k_2^{\text{ca}} + k_3^{\text{ca}} + k_4^{\text{ca}} + k_5^{\text{ca}}}$$

for  $i = 2-5$ . The rate constants here refer to the chemically activated system described above, not the reactions in Table 1. A plot of these branching ratios vs pressure from the master-equation calculations at a temperature of 1100 K is presented in Figure 3. We see that these branching ratios change relatively little over a wide pressure range. We may also compare them to the effective branching ratios at the high pressure defined above. At 1100 K these are  $B_{2,\infty} = 0.828$ ,  $B_{3,\infty} = 0.042$ ,  $B_{4,\infty} = 0.087$ ,  $B_{5,\infty} = 0.043$ . These are essentially the same as the values shown in Figure 3 at low pressures. This suggests that the total branching ratios, a combination of recombination followed by dissociation and direct chemically activated reaction, will be roughly constant at all pressures. This means that using the high-pressure recombination and dissociation rate constants will reasonably describe the reactions even at low pressures. We have only shown this for one of the reactions in the mechanism ( $\text{SiH}_2\text{Cl}_2 + \text{SiHCl}$ ). A rigorous analysis would require performing master-equation calculations for the multi-channel decomposition reactions 6–33 of the mechanism and analyzing chemically activated reactions, as done here for one case, for the reverse of reactions 6–32. Description of these chemically activated reactions would add 60 additional pressure-dependent elementary reactions to the mechanism. The analysis

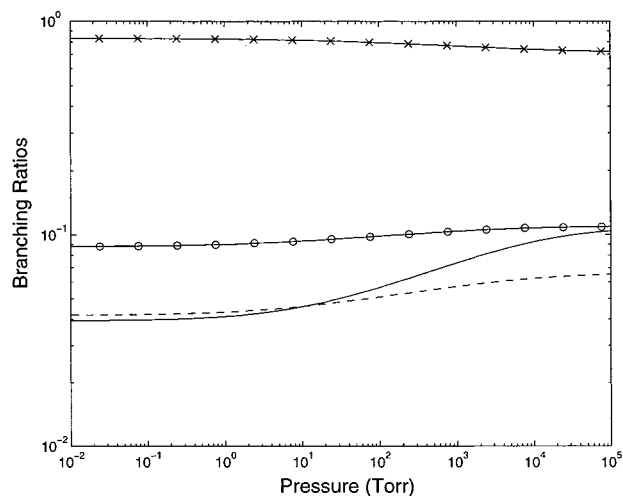


**Figure 3.** Branching ratios for the chemically activated system, as defined in the text. The  $\times$ 's are  $B_2$ , the dashed line is  $B_3$ , the  $\circ$ 's are  $B_4$ , and the solid line is  $B_5$ .

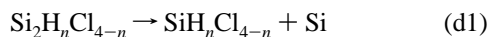
presented above suggests that we can avoid this and capture the essence of the behavior of this system using the high-pressure rate parameters as has been done here. It should be emphasized that this will only work under conditions where the chlorinated disilanes are not present initially and decompose rapidly so that their concentrations always remain small compared with the concentrations of the major species in the system. If significant quantities of these species are present, then the more rigorous treatment will be required.

**Reactions Involving the Chlorinated Disilenes and Silylsilylenes.** Reactions 34–39 are decomposition of the chlorinated disilenes and silylsilylenes and their reverse reactions, dimerization of the chlorinated silylenes. In this work, we have included a single species for each stoichiometry  $\text{Si}_2\text{H}_n\text{Cl}_{4-n}$  with the properties of the lowest-energy isomer. For  $\text{Si}_2\text{H}_4$ , this is disilene ( $\text{H}_2\text{SiSiH}_2$ ), which is about 7 kcal/mol lower in energy than silylsilylene ( $\text{H}_3\text{SiSiH}$ ).<sup>29</sup> For the molecules containing one or more chlorines, however, our ab initio calculations<sup>30</sup> predict that the lowest-energy isomer is always the chlorinated silylsilylene isomer with a chlorine atom attached to the divalent silicon atom ( $\text{H}_n\text{Cl}_{3-n}\text{SiSiCl}$ ). Isomerization between the different isomers is very fast compared with the other reactions. The activation energy for isomerization of  $\text{H}_3\text{SiSiH}$  to  $\text{H}_2\text{SiSiH}_2$  was calculated by Gordon et al.<sup>31</sup> to be 9 kcal/mol (corresponding to 16 kcal/mol for the reverse reaction). We have calculated barriers (electronic plus zero-point energy) ranging from 5 to 23 kcal/mol above the disilene structure for the isomerizations of the chlorinated disilenes to silylsilylenes by H or Cl transfer.<sup>31</sup> These reactions will clearly be much faster than the other unimolecular reactions in the mechanism, with the exception of reaction 39 where the isomerization barrier is only a few kcal/mol below the decomposition barrier and dissociation may compete with isomerization. At ordinary pressures (less than a few atmospheres) and temperatures high enough that the overall decomposition takes place on a reasonable time scale (seconds or less), they will also be faster than any of the bimolecular reactions. It is therefore reasonable to assume that these isomerizations come to rapid equilibrium and that each species can be represented by only its lowest-energy isomer. The dimerization of two divalent chlorinated silylenes (the reverse of reactions 34–39) is expected to be barrierless, and this was confirmed by ab initio calculations.<sup>30</sup> We therefore take the activation energy for decomposition to be simply the heat of reaction at 1000 K and use a preexponential factor of

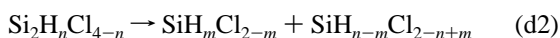
$10^{15}$  for the decomposition reactions 35–40. This is taken as a typical preexponential for unimolecular decomposition via a loose transition state. More realistic treatment of these reactions would require variational transition-state theory calculations based on interaction potentials between the reactants that are currently not known. The pressure dependence of these reactions is also neglected. They are certainly in the pressure-dependent regime, but their absolute rates turn out to be unimportant for the cases considered here. For the most part they are much faster than other steps in the mechanism and rapidly approach equilibrium. Increasing or decreasing the preexponential factor for reactions 34–39 in both directions by an order of magnitude (leaving the equilibrium constant unchanged) had only small effects on the results of simulations of homogeneous decomposition of the chlorinated silanes. It should be emphasized that the presence of these reactions in the mechanism is essential, since they generate and consume the chlorinated silylenes and play an important role in determining the concentrations of these reactive species.

**Reactions Leading to Silicon Atom Formation.** We have not included any reactions that would lead to silicon atom formation. Ho and Breiland<sup>32</sup> observed silicon atoms in CVD from dichlorosilane by laser-induced fluorescence, but concentrations were much smaller than during CVD from silane.  $H_2$  elimination from  $SiH_2$  is about 44 kcal/mol endothermic at 1000 K. Even if this reaction has no additional activation barrier, it is still predicted to be too slow to compete with the insertion reactions of  $SiH_2$  into hydrogen and the chlorinated silanes. In the mechanism for gas-phase chemistry in CVD of silicon from silane presented by Ho et al.,<sup>10</sup> the primary source of silicon atoms is the reaction  $H_3SiSiH \rightarrow SiH_4 + Si$ . Analogous reactions that eliminate a silicon atom from  $Si_2H_nCl_{4-n}$  to give a chlorinated silane (i.e.,  $Si_2H_2Cl_2 \rightarrow SiH_2Cl_2 + Si$ ) are 47–50 kcal/mol endothermic at 1000 K. The height of any additional activation barrier is not known. If there were no barrier for the reverse reaction, then these decompositions could compete with decomposition to silylenes for  $Si_2H_4$  and  $Si_2H_3Cl$  (reactions 34 and 35) but not for the more chlorinated compounds (reactions 36–39).

This provides an explanation for the much lower densities of silicon atoms in CVD from dichlorosilane than in CVD from silane. As seen above, the competing processes for decomposition of  $Si_2H_nCl_{4-n}$  are elimination of a silicon atom or decomposition to two silylenes:



or



The endothermicity of the first channel (eq d1) remains relatively constant with chlorine substitution (47–50 kcal/mol). However, as seen in Table 1, the endothermicity of the second reaction (eq d2) decreases strongly with chlorine substitution, from 61 kcal/mol for  $Si_2H_4 \rightarrow 2SiH_2$  to only 23 kcal/mol for  $Si_2Cl_4 \rightarrow 2SiCl_2$ . This large change in enthalpy of reaction can be attributed to the substantial increase in stability in going from  $SiH_2$  to  $SiHCl$  to  $SiCl_2$ , the products of the second reaction path. As discussed above, the second reaction type (eq d2) should be barrierless and should have a large preexponential factor. In deposition from silane, no chlorine is present, so  $Si_2H_4$  is formed and its decomposition by the first channel (eq d1) may be an important source of silicon atoms, as predicted by Ho et al.<sup>10</sup> However, in deposition from dichlorosilane, the more chlori-

nated species  $Si_2H_2Cl_2$ ,  $Si_2HCl_3$ , and  $Si_2Cl_4$  are formed. For these compounds, the second reaction path (eq d2) will dominate. Thus, silicon atom formation is suppressed in CVD from dichlorosilane because the lower-energy path (eq d2) that leads to silylenes instead of silicon atoms is available for decomposition of the more chlorinated reaction intermediates  $Si_2H_2Cl_2$ ,  $Si_2HCl_3$ , and  $Si_2Cl_4$ . Since we are only considering decomposition of the chlorinated silanes, reactions of the second type (eq d2) are included in this mechanism, while reactions of the first type (eq d1) are not.

**Reactions with HCl.** Finally, we have not included insertions of the  $Si_2H_nCl_{4-n}$  species into HCl or the chemically activated reactions  $SiHCl + HCl \rightarrow SiH_2Cl_2^* \rightarrow SiCl_2 + H_2$  and  $SiH_2 + HCl \rightarrow SiH_3Cl^* \rightarrow SiHCl + H_2$ . The chlorinated silylenes have smaller barriers for insertion into HCl than for insertion into  $H_2$ . Therefore, the chlorinated silylsilylenes might also insert into HCl more readily than into  $H_2$ . For the conditions considered here, decomposition in excess  $H_2$  with no source of HCl other than production by reactions 3, 4, and 6, the HCl concentration is always small and we can safely neglect these reactions with HCl. However, in a CVD process operating at high reactant utilization so that large amounts of HCl were produced, or in a process where HCl was added as a reactant to achieve selective growth, we would also want to consider these reactions with HCl. In the present case, however, this would unnecessarily complicate the mechanism without significantly affecting the results.

The reaction mechanism described here is intended to qualitatively capture the most important elements in the multistep thermal decomposition of  $SiH_3Cl$ ,  $SiH_2Cl_2$ , and  $SiHCl_3$  with as much realism as possible given the lack of experimental information on the elementary reactions in this system. A key feature is that it has been developed self-consistently based on sets of ab initio calculations with a uniform treatment for competing reactions. This means that relative reaction rates should be more accurate than the absolute rates, which have uncertainties due to uncertainties in the calculated barrier heights and the calculated preexponential factors. The mechanism includes the type of silylene-mediated chain mechanisms described in the Introduction, which appear to be the most important secondary chemistry occurring in this system. It also captures the bulk of the pressure dependence of the overall decomposition by explicitly treating the pressure dependence of the initiating chlorinated silane unimolecular decompositions. In the almost complete absence of experimental information on homogeneous reactions in this system, this gives us a means of ascertaining which, if any, reactions are likely to be important under given conditions and provides a framework in which to conduct experimental studies as further investigation is warranted.

### Comparison with Experimental Observations

Simulations of isothermal, homogeneous decomposition of  $SiH_3Cl$ ,  $SiH_2Cl_2$ , and  $SiHCl_3$  have been carried out to investigate the implications of the mechanism presented here and to identify the most important reaction paths. We simply state key results for dichlorosilane decomposition here and will present the details of these simulations and their implications for silicon epitaxy in a separate publication. It was found that the rate of dichlorosilane decomposition predicted by the full mechanism was dramatically increased compared with the rate of unimolecular decomposition alone. For 1% dichlorosilane in 100 Torr of  $H_2$ , the decomposition was accelerated by a factor of about 270 at 800 K, declining to a factor of about 5 at 1300 K. The

extent of this acceleration, of course, also depends on the initial concentration of dichlorosilane and the total pressure. Examination of reaction rates and sensitivity analysis showed that this acceleration was due to chain reactions propagated by SiH<sub>2</sub>, SiHCl, and SiCl<sub>2</sub>. The SiH<sub>2</sub>-propagated chain consisting of reactions -14, 17, and 36 in Table 1 was the fastest path for dichlorosilane consumption under conditions considered, but analogous cycles involving SiHCl and SiCl<sub>2</sub> also contributed significantly. We remind the reader that there is uncertainty in the calculated rate parameters for silylene-elimination reactions such as reaction 14 due to the use of a tight transition state in calculating the rate parameters. Thus, the calculated activation energies are lower than one might expect but appear reasonable at these high temperatures. As the temperature increases, the apparent activation energy decreases owing to a tightening of the transition state. Thus, one expects somewhat lower activation energies under conditions considered here than at the lower temperatures where these reactions are often studied. The predicted apparent activation energy for the overall dichlorosilane decomposition was much lower than the activation energy for unimolecular decomposition. Almost all of the SiHCl produced by unimolecular decomposition was converted to SiCl<sub>2</sub> by the secondary reactions so that the dominant products were SiCl<sub>2</sub> and H<sub>2</sub> at temperatures above 1000 K, along with SiH<sub>3</sub>Cl and SiHCl<sub>3</sub> at lower temperatures. The fastest path for dichlorosilane consumption was reaction with SiH<sub>2</sub>, but reaction with SiHCl and reaction with SiCl<sub>2</sub> also consumed significant quantities.

The predictions of the mechanism presented here are generally consistent with the experimental observations on dichlorosilane decomposition mentioned in the Introduction and can explain some of the apparent discrepancies and reconcile the experimental results with the ab initio calculations. Our simulations predict that SiCl<sub>2</sub> and H<sub>2</sub> are the principle products of the overall homogeneous reaction, even though the elementary unimolecular decomposition of dichlorosilane produces SiHCl and HCl as predicted by the ab initio calculations.<sup>12,13</sup> The homogeneous production of large concentrations of SiCl<sub>2</sub> predicted by this mechanism is consistent with the mass-spectrometric observations of Ban and Gilbert.<sup>8</sup> Likewise, the small quantities of SiHCl predicted would be detectable by the laser-induced fluorescence techniques used by Ho and Brieland<sup>9</sup> to observe that species. The observation of Walker et al.<sup>6</sup> that HCl was produced in quantities much smaller than the amount of SiH<sub>2</sub>-Cl<sub>2</sub> consumed in both static pyrolyses and shock-tube experiments is also consistent with our predictions, since our mechanism leads to SiCl<sub>2</sub> and H<sub>2</sub> as the dominant products, even though the primary dissociation is to SiHCl and HCl. Since, at this writing, the work of Walker et al. has not yet appeared in print, we have not attempted a detailed comparison of our predictions with their product yields. Surface reactions, which are not considered here, clearly also played an important role in their experiments. The mechanism presented here is also compatible with the rate parameters measured in our laser pyrolysis experiments,<sup>11</sup> since at the high temperatures of those experiments (1350–1700 K) the secondary reactions would contribute little and rate parameters close to those for unimolecular decomposition would be obtained. We cannot as readily explain the observation of electronically excited SiCl<sub>2</sub> in the multiphoton dissociation experiments of Sausa and Ronn.<sup>5</sup> The absence of significant quantities of HCl as a final product in their experiments and the presence of H<sub>2</sub> as a product could be explained by the secondary chemistry described here. However, they observed emission from electronically excited SiCl<sub>2</sub> under

effectively collisionless conditions where the SiCl<sub>2</sub> could not have been produced by secondary reactions. It is possible that the emission they observed was from the small fraction of dichlorosilane that dissociates to SiCl<sub>2</sub> and H<sub>2</sub> or that multiphoton absorption gives a nonthermal distribution of reactant energies that favors decomposition to SiCl<sub>2</sub> and H<sub>2</sub>. With this one exception, however, the mechanism presented here appears to reconcile the various experimental observations on dichlorosilane decomposition with the predictions of the ab initio calculations.<sup>14,15</sup>

## Summary and Conclusions

A mechanism for homogeneous decomposition of the chlorinated silanes (SiH<sub>3</sub>Cl, SiH<sub>2</sub>Cl<sub>2</sub>, and SiHCl<sub>3</sub>) with rate parameters based self-consistently on ab initio molecular-orbital calculations has been presented. This mechanism predicts that thermal decomposition of dichlorosilane is accelerated by chain reactions propagated by SiH<sub>2</sub>, SiHCl, and SiCl<sub>2</sub> and that secondary reactions convert SiHCl produced by unimolecular decomposition of dichlorosilane to SiCl<sub>2</sub>. These results are consistent with experimental observations of dichlorosilane decomposition and reconcile them with predictions of ab initio calculations for the unimolecular decomposition of dichlorosilane.

**Acknowledgment.** This work was partially supported by the National Science Foundation under Grant CTS-9504827. M.T.S. thanks the University of Minnesota for support in the form of a doctoral dissertation fellowship. We are very grateful to Dr. Prasana Venkatesh for performing the master-equation calculations on the chemically activated reaction system described above.

## References and Notes

- (1) Ring, M. A.; O'Neal, H. E. *J. Phys. Chem.* **1992**, *96*, 10848.
- (2) Ho, P.; Coltrin, M. E.; Breiland, W. G. *J. Phys. Chem.* **1994**, *98*, 10138.
- (3) Becerra, R.; Walsh, R. *J. Phys. Chem.* **1992**, *96*, 10856.
- (4) Lavrushenko, B. B.; Baklanov, A. V.; Strunin, V. P. *Spectrochim. Acta* **1990**, *46A*, 479.
- (5) Sausa, R. C.; Ronn, A. M. *Chem. Phys.* **1985**, *96*, 183.
- (6) Walker, K. W.; Jardine, R. E.; Ring, M. A.; O'Neal, H. E. *Int. J. Chem. Kinet.*, in press.
- (7) Kruppa, G. H.; Shin, S. K.; Beauchamp, J. L. *J. Phys. Chem.* **1990**, *94*, 327.
- (8) Ban, V. S.; Gilbert, S. L. *J. Electrochem. Soc.* **1975**, *122*, 1382.
- (9) Ho, P.; Breiland, W. G. *Appl. Phys. Lett.* **1983**, *43*, 125.
- (10) Ho, P.; Breiland, W. G.; Carr, R. W. *Chem. Phys. Lett.* **1986**, *132*, 422.
- (11) Swihart, M. T.; Carr, R. W. *J. Electrochem. Soc.* **1997**, *144*, 4357.
- (12) Su, M.-D.; Schlegel, H. B. *J. Phys. Chem.* **1993**, *97*, 9981.
- (13) Wittbrodt, J. M.; Schlegel, H. B. *Chem. Phys. Lett.* **1997**, *265*, 527.
- (14) Su, M.-D.; Schlegel, H. B. *J. Phys. Chem.* **1993**, *97*, 8732.
- (15) Swihart, M. T.; Carr, R. W. *J. Phys. Chem. A* **1997**, *101*, 7434.
- (16) McQuarrie, D. A. *Statistical Mechanics*; Harper Collins: New York, 1976; Chapter 8.
- (17) Chase, M. W.; Davies, C. A.; Downey, J. R.; Frurip, D. J.; McDonald, R. A.; Szverud, A. N. JANAF Thermochemical Tables, 3rd ed. *J. Phys. Chem. Ref. Data* **1985**, *14*.
- (18) Gilbert, R. G.; Smith, S. C.; Jordan, M. J. T. UNIMOL program suite (calculation of falloff curves for unimolecular and recombination reactions), 1993. Available from the authors at School of Chemistry, Sydney University, NSW 2006, Australia, or by e-mail to gilbert-r@summer.chem.su.oz.au.
- (19) Oref, I.; Tardy, D. C. *Chem. Rev.* **1990**, *90*, 1407.
- (20) Tardy, D. C.; Rabinovitch, B. S. *Chem. Rev.* **1977**, *77*, 369.
- (21) Holbrook, K. A.; Piling, M. J.; Robertson, S. H. *Unimolecular Reactions*, 2nd ed.; John Wiley and Sons: Chichester, England, 1996.
- (22) Gilbert, R. G.; Smith, S. C. *Theory of Unimolecular and Recombination*

bination Reactions; Blackwell Scientific Publications: Oxford, England, 1990.

(23) Gilbert, R. G.; Luther, K.; Troe, J. *Ber. Bunsenges. Phys. Chem.* **1983**, *87*, 169. The unimolecular rate constant is obtained as  $k_{\text{uni}} = k_{\infty}[p^*/(1 + p^*)]F(p^*)$ , where  $p^* = k_0[M]/k_{\infty}$ ,  $[M] =$  total concentration,  $k_0 =$  low-pressure-limiting rate constant  $= A_0 \exp[-E_0/(RT)]$ ,  $k_{\infty} =$  high-pressure-limiting rate constant  $= A_{\infty} \exp[-E_{\infty}/(RT)]$ ,  $\log[F(p^*)] = (\log F_{\text{cent}})/\{1 + [(\log p^* + c)/(N - d(\log p^* + c))]^2\}$ ,  $c = -0.4 - 0.67 \log F_{\text{cent}}$ ,  $N = 0.75 - 1.27 \log F_{\text{cent}}$ ,  $d = 0.14$ ,  $F_{\text{cent}} = \exp(-T/T^{**}) + \exp(-T^*/T)$ .

(24) Jasinski, J. M.; Becerra, R.; Walsh, R. *Chem. Rev.* **1995**, *95*, 1203.

(25) Moffat, H. K.; Jensen, K. F.; Carr, R. W. *J. Phys. Chem.* **1991**, *95*, 145.

(26) Steinfeld, J. I.; Francisco, J. S.; Hase, W. L. *Chemical Kinetics and Dynamics*; Prentice Hall; Englewood Cliffs, NJ, 1989.

(27) Venkatesh, P. K.; Dean, A. M.; Cohen, M. H.; Carr, R. W. *J. Chem. Phys.*, in press.

(28) Venkatesh, P. K.; Dean, A. M.; Cohen, M. H.; Carr, R. W. *J. Chem. Phys.*, to be submitted.

(29) Curtiss, L. A.; Raghavachari, K.; Deutsch, P. W.; Pople, J. A. *J. Chem. Phys.* **1991**, *95*, 2433.

(30) Swihart, M. T.; Carr, R. W. *J. Phys. Chem.*, in press.

(31) Gordon, M. S.; Truong, T. N.; Bonderson, E. K. *J. Am. Chem. Soc.* **1986**, *108*, 1421.

(32) Ho, P.; Breiland, W. G. *J. Appl. Phys.*, **1988**, *63*, 5184.